AD-A115 144 CALIFORNIA UNIV LOS ANGELES DEPT OF ELECTRICAL SCIEN--ETC F/G 20/6
ACCURACY OF DIRECTIONAL COUPLER THEORY IN FIBER OR INTEGRATED O--ETC(U)
SEP 78 C YEH, F MANSHADI, K F CASEY N00014-76-C-0321

UNCLASSIFIED NL

END
DATE FILMED
7-82
DTIC

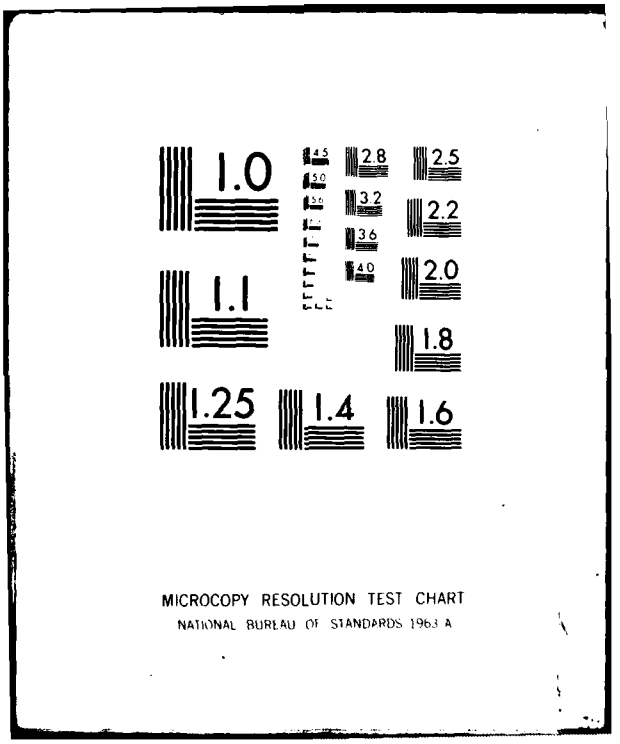
1.0
1.1
1.25
1.4
1.6
1.8
2.0
2.2
2.5
2.8
3.2
3.6
4.0
4.5
5.0
5.6
MICROCOPY RESOLUTION TEST CHART
NATIONAL BUREAU OF STANDARDS 1963 A

(1)

ACCURACY OF DIRECTIONAL COUPLER THEORY IN FIBER OR INTEGRATED OPTICS APPLICATIONS†

371-089

C. Yeh, F. Manshadi, K. F. Casey* and A. Johnston**

Electrical Sciences and Engineering Department
University of California, Los Angeles
Los Angeles, California 90024

SEPT-1978

Based on the solution of a simplified canonical problem, the possible margin of error on the predicted coupling length according to the coupled mode theory as applied to fiber and integrated optical guides is inferred. It was found that coupling length obtained according to the coupled mode theory is usually accurate to within 20% of the actual value provided that the frequency of operation is above the cutoff frequency of the antisymmetric mode of the coupled structure.

N00014-76-C-0321

* K. F. Casey is with the Department of Electrical Engineering, Kansas State University, Manhattan, Kansas.

** A. Johnston is with the Jet Propulsion Laboratories, Pasadena, California 91103.

† Partly supported by ONR.

This document has been approved for public release and sale; its distribution is unlimited.

Coupled mode theory has been used extensively in recent years in the analysis of many important problems in integrated optics and fiber optics.[1-3] It is therefore of extreme interest to learn the region of validity for which the coupled mode theory will yield accurate results. Since exact solutions for most practical problems are not available, we shall therefore deal specifically with a canonical problem whose exact solution, as well as approximate solution based on the coupled mode theory, is obtainable. Comparison of the results may then provide an indication of the accuracy of the coupled mode theory approach. It is shown that when the coupled mode theory is used properly, the prediction of coupling distances is surprisingly accurate even when the separation between the guides is relatively small. However, as far as the field configurations of coupled guides are concerned, significant inaccuracy is observed when the separation distance becomes small.

The geometry of the problem is shown in Fig. 1. Two identical dielectric slab waveguides are located in the regions $d/2 \leq |x| \leq a+d/2$. The permittivity of the slab guides is ε_1 and that of the regions outside the guides is ε_2; furthermore, $\varepsilon_1 > \varepsilon_2$. The permeability is assumed to be μ_o everywhere. A perfectly conducting plane covers the surface $z = 0$ except for the region $d/2 \leq x \leq a+d/2$. In that aperture, the tangential electric field is $E_o \bar{a}_x$. All electromagnetic field quantities are independent of the coordinate y and the time dependence $\exp(j\omega t)$ is assumed and suppressed.

The electromagnetic field has components E_x, E_z and H_y, which are related as

$$E_x = \frac{-1}{j\omega\varepsilon} \frac{\partial H_y}{\partial z} \tag{1a}$$

$$E_z = \frac{1}{j\omega\varepsilon} \frac{\partial H_y}{\partial x} \tag{1b}$$

H_y satisfies

$$\frac{\partial^2 H_y}{\partial x^2} + \frac{\partial^2 H_y}{\partial z^2} + k_i^2 H_y = 0 \tag{2}$$

where $k_i^2 = \omega^2 \mu_o \varepsilon_i$, $i = 1,2$. Now it is necessary to specify that all field components have the same z-dependence, i.e., $\exp(-j\beta z)$. Thus if $E_x(x,z) = \hat{E}_x(x)\exp(-j\beta z)$ and similarly for E_z and H_y, we have

$$\hat{E}_x = \frac{\beta}{\omega\varepsilon} \hat{H}_y \tag{3a}$$

$$\hat{E}_z = \frac{1}{j\omega\varepsilon} \frac{d\hat{H}_y}{d_x} \tag{3b}$$

$$\frac{d^2\hat{H}_y}{dx^2} + (k_i^2 - \beta^2)\hat{H}_y = 0 \tag{3c}$$

We are concerned with the excitation by the aperture field of the guided modes on this structure; the guided-wave field will be the dominant portion of the total field for large z. Solutions of Eq. (3c) corresponding to the guided-wave field are

$$-\infty \le x \le -a-d/z: \quad \hat{H}_{yn}^{(1)}(x) = A_n \exp[v_n(x+a+d/2)] \tag{4a}$$

$$-a-d/2 \le x \le -d/2: \quad \hat{H}_{yn}^{(2)}(x) = B_n \sin u_n(x+d/2) + C_n \cos u_n(x+d/2) \tag{4b}$$

$$-d/2 \le x \le d/2: \quad \hat{H}_{yn}^{(3)}(x) = D_n \sinh v_n x + E_n \cosh v_n x \tag{4c}$$

$$d/2 \le x \le a + d/2: \quad \hat{H}_{yn}^{(4)}(x) = F_n \sin u_n(x-d/2) + G_n \cos u_n(x-d/2) \tag{4d}$$

$$a + d/2 \le x \le \infty: \quad \hat{H}_{yn}^{(5)}(x) = H_n \exp[-v_n(x-a-d/2)] \tag{4e}$$

in which $u_n^2 = k_1^2 - \beta_n^2$, $v_n^2 = \beta_n^2 - k_2^2$, and the coefficients $A_n - H_n$ are to be determined. The "n" subscripts refer to the nth guided-wave mode.

The characteristic equation from which the values of β_n may be determined is found by forcing the tangentical field components E_z and H_y to be continuous at the four dielectric interfaces. By virtue of the symmetry of the configuration about $x = 0$, the electromagnetic field may be separated into two parts whose axial electric field E_z has either even or odd symmetry about $x = 0$. For the even modes, $H_n = -A_n$, $G_n = -C_n$, $F_n = B_n$, and $E_n = 0$; for the odd modes, $H_n = A_n$, $G_n = C_n$, $F_n = -B_n$, and $D_n = 0$. Thus considering the two cases separately, one matches the boundary conditions at $x = d/2$ and $x = a + d/2$, and obtains

$$\left[\tan u_n a - \frac{2qu_n v_n}{q^2u_n^2 - v_n^2 + (q^2u_n^2 + v_n^2)\exp(-v_n d)}\right] \cdot$$

$$\left[\tan u_n a - \frac{2qu_n v_n}{q^2u_n^2 - v_n^2 - (q^2u_n^2 + v_n^2)\exp(-v_n d)}\right] = 0 \qquad (5)$$

in which $q = \varepsilon_2/\varepsilon_1$. The roots of the first factor in square brackets yield the even modes; those of the second factor, the odd modes.

We may also evaluate the coefficients $A_n - H_n$ in terms of any single one of them, say A_n. The relationship is expressed as $B_n = b_n A_n, \ldots, H_n = h_n A_n$ in which $b_n - h_n$ are given by

<u>even modes</u>:

$$b_n^e = f_n^e = \frac{1}{\Delta_n^e}\frac{v_n}{\varepsilon_2}\cosh\frac{v_n d}{2} \qquad (6a)$$

$$c_n^e = -g_n^e = -\frac{1}{\Delta_n^e}\frac{u_n}{\varepsilon_1}\sinh\frac{v_n d}{2} \qquad (6b)$$

$$d_n^e = \frac{1}{\Delta_n^e}\frac{u_n}{\varepsilon_1}, \quad e_n^e = 0, \quad h_n^e = -1 \qquad (6c)$$

$$\Delta_n^e = \frac{-v_n}{\varepsilon_2}\cosh\frac{v_n d}{2}\sin u_n a - \frac{u_n}{\varepsilon_1}\sinh\frac{v_n d}{2}\cos u_n a \qquad (6d)$$

odd modes:

$$b_n^o = -f_n^o = \frac{1}{\Delta_n^o}\frac{v_n}{\varepsilon_2}\sinh\frac{v_n d}{2} \tag{7a}$$

$$c_n^o = g_n^o = -\frac{1}{\Delta_n^o}\frac{u_n}{\varepsilon_1}\cosh\frac{v_n d}{2} \tag{7b}$$

$$d_n^o = 0,\quad e_n^o = -\frac{1}{\Delta_n^o}\frac{u_n}{\varepsilon_1},\quad h_n^o = 1 \tag{7c}$$

$$\Delta_n^o = -\frac{v_n}{\varepsilon_2}\sinh\frac{v_n d}{2}\sin u_n' a - \frac{u_n}{\varepsilon_1}\cosh\frac{v_n d}{2}\cos u_n a \tag{7d}$$

This completes the formal analysis of the guided-mode electromagnetic field on the dual slab waveguide structure.

We now consider the boundary condition at $z = 0$, i.e., that $E_x(x,o) = E_o$ for $d/2 \le x \le a + d/2$ and $E_x(x,o) = 0$ elsewhere. Equating the excitation field to the total field E_x for $z \ge 0$ at $z = 0$ yields

$$E_o\left[U(x-d/2) - U(x-a-d/2)\right] = \sum_n \frac{-\beta_n}{\omega\varepsilon(x)}\hat{H}_{yn}(x) + (\text{radiated field})\Big|_{x=0} \tag{8}$$

where U is the unit step function. The sum is taken over the guided modes for which β_n is a proper root† of Eq. (5). By virtue of the orthogonality relation

$$\int_{-\infty}^{\infty}\frac{1}{\varepsilon(x)}\hat{H}_y(x;\beta)\hat{H}_y^*(x;\beta')dx = 0 \quad (\beta \neq \beta') \tag{9}$$

we readily obtain

†i.e., a root for which $\mathrm{Re}(v_n) \ge 0$.

$$-\frac{\omega}{\beta_n} E_o \int_{d/2}^{a+d/2} \hat{H}_{yn}^{(4)*}(x)\,dx = \frac{1}{\varepsilon_2}\int_{-\infty}^{-a-d/2} |\hat{H}_{yn}^{(1)}(x)|^2\,dx + \frac{1}{\varepsilon_1}\int_{-a-d/2}^{-d/2} |\hat{H}_{yn}^{(2)}(x)|^2\,dx$$

$$+\frac{1}{\varepsilon_2}\int_{-d/2}^{d/2} |\hat{H}_{yn}^{(3)}(x)|^2\,dx + \frac{1}{\varepsilon_1}\int_{d/2}^{a+d/2} |\hat{H}_{yn}^{(4)}(x)|^2\,dx$$

$$+\frac{1}{\varepsilon_2}\int_{a+d/2}^{\infty} |\hat{H}_{yn}^{(5)}(x)|^2\,dx + (\text{radiated fields}) \qquad (10)$$

The integrals in Eq. (10) are easily evaluated and yield a relation between E_o and A_n. We find that

$$A_n = \frac{-\omega E_o}{u_n \beta_n}\left[f_n^*(1-\cos u_n a) + g_n^* \sin u_n a\right] \cdot \left\{\frac{1}{v_n \varepsilon_2}\right. \qquad (11)$$

$$+\frac{1}{u_n \varepsilon_1}\left[|g_n|^2(u_n a + \tfrac{1}{2}\sin 2u_n a) + |f_n|^2(u_n a - \tfrac{1}{2}\sin 2u_n a)\right.$$

$$\left.\left. + (f_n g_n^* + f_n^* g_n)\sin^2 u_n a\right] + \frac{u_n^2}{2\Delta_n^2 v_n \varepsilon_1^2 \varepsilon_2}(\sinh v_n d \pm v_n d)\right\}^{-1}$$

in which the lower (-) sign is taken for the even modes, and the upper (+) sign for the odd modes. Δ_n^2 is either Δ_n^{e2} or Δ_n^{o2} as appropriate, as are f_n and g_n. This completes the formal solution for the excitation of the guided-wave field by the aperture electric field at z = 0. Here we have assumed that the contribution of the exciting field to the radiated field is negligible as compared with the guided field.

We now consider the special case which is of particular interest for the purposes of this paper, that in which only a single mode is possible on each of the dielectric slabs in isolation. We shall further require that the lowest-order even and odd modes will propagate on the dual-guide structure.

Thus,

$$\frac{2a}{qd} < ua \tan ua < \infty$$

where $0 < ua < \pi/2$. We now evaluate the z-component of the Poynting vector in each of the slab waveguides under the assumption that only these lowest-order modes exist; their propagation constants are denoted β_e and β_o, and the associated fields $\hat{H}_y(x)$ are denoted $\hat{H}_{ye}(x)$ and $\hat{H}_{yo}(x)$ respectively. In the "upper" guide ($d/2 < x < a+d/2$) or "guide A", we have

$$P_{zA}(x,z) = \frac{1}{2\omega}\mathrm{Re}\left\{\frac{1}{\varepsilon_1}\left[\beta_e|\hat{H}_{ye}^{(4)}(x)|^2 + \beta_o|\hat{H}_{yo}^{(4)}(x)|^2 + \beta_e\hat{H}_{ye}^{(4)}(x)\hat{H}_{yo}^{(4)*}(x)e^{-j(\beta_e-\beta_o^*)z} + \beta_o\hat{H}_{yo}^{(4)}(x)\hat{H}_{ye}^{(4)*}(x)e^{j(\beta_e^*-\beta_o)z}\right]\right\} \tag{12}$$

In the "lower" guide, or "guide B",

$$P_{zB}(x,z) = \frac{1}{2\omega}\,\mathrm{Re}\left\{\frac{1}{\varepsilon_1}\left[\beta_e|\hat{H}_{ye}^{(2)}(x)|^2 + \beta_o|\hat{H}_{yo}^{(2)}(x)|^2 + \beta_e\hat{H}_{ye}^{(2)}(x)\hat{H}_{yo}^{(2)*}(x)e^{-j(\beta_e-\beta_o^*)z} + \beta_o\hat{H}_{yo}^{(2)}(x)\hat{H}_{ye}^{(2)*}(x)e^{-j(\beta_e^*-\beta_o)z}\right]\right\} \tag{13}$$

We may now calculate the total power per unit width carried in each of the slab waveguides† by integrating P_{zA} from $x = d/2$ to $x = a+d/2$ and P_{zB} from $x = -a-d/2$ to $x = -d/2$. Denoting these powers by P_A and P_B, we obtain,

†The power carried outside the slab guides is not included in the calculation. Thus P_A and P_B will not reduce to the total power carried in a single slab waveguide mode in the limit $d \to \infty$.

assuming that ε_1, ε_2, β_e, and β_o are purely real,

$$P_A(z) = \int_{d/2}^{a+d/2} P_{zA}(x,z)dx, \quad P_B(z) = \int_{-a-d/2}^{-d/2} P_{zB}(x,z)dx$$

Now we are in a position to compute exactly how the input power is transferred from one guide to the other. (The only assumption is that no radiated power is present.) We must first determine the propagation constants of the guided modes along the slabs from Eq. (5). Results for the two lowest order modes are displayed in Fig. 2 for the symmetric modes and in Fig. 3 for the anti-symmetric modes. In these figures, the normalized propagation constant β/k_o is plotted against the normalized thickness of the slab $k_o a$ for various values of the normalized separation of the slabs $k_o d$. The constant k_o, the free-space wave number, is defined as $\omega\sqrt{\mu_o \varepsilon_o}$. It can be seen that there exists no cutoff frequency for the lowest order symmetric mode while a cutoff frequency does exist for the lowest order anti-symmetric mode. Of course, all higher order symmetric and anti-symmetric modes possess cutoff frequencies.

To illustrate how the guided power exchanges between the two guiding structures, Figs. 4-5 are introduced. The operating frequency is so selected that only the dominant symmetric mode and the lowest order antisymmetric mode may exist along the guiding structure. It is interesting to note that although the initial exciting field exists only at the entrance of the core region of guide A, according to our computed results there exists a small amount of guided power in guide B. The reason for this is that to satisfy the initial given field configuration at the entrance of the guiding structure, radiation mode as well as guided modes must be taken into account. Since we have á priori ignored the radiation mode in our calculation, we can only satisfy approximately

the given initial field. The quantity P_B at $z = 0$ represents the power calculated from the field that extends from guide A into the core region of guide B. It can also be seen from these figures that guided power exchanges from one guide to the other in a periodic fashion as expected. The distance for which maximum guided power is transferred from one guide to the other is called the coupling length. It is noted that the coupling length becomes shorter as the separation distance between the guides is shortened. To correlate the maximum power contained in the core region of guide A with the normalized separation distance $k_o d$, we have performed the computation at the entrance of the coupled guide. Results are shown in Fig. 6. It can be seen that the normalized maximum power in the core region of guide A varies in a rather unusual fashion for small separation distances. At large $k_o d$, the maximum power contained in the core region approaches that for the case of an isolated slab guide, as expected. To further understand the behavior of the transverse fields in the guides when the separation distance is small, we have plotted in Fig. 7 the quantity $|E_x|$ vs. the transverse distance. The complexity of the evolution of the transverse electric field as the separation distances are changed indicates the complex nature of the curves in Fig. 6 when the separation distances are small.

Recall that the primary purpose of our investigation is to determine how accurate the coupled mode theory is in its treatment of the coupled dielectric waveguide problem. We have carried out the cases treated above according to the coupled mode theory described by Marcuse[1] and by NELC researchers.[2] The "exact" normal mode results are then compared with those obtained according to the various coupled-mode theories. Displayed in Fig. 8 are the curves for the coupling length as a function of the normalized separation distance between two parallel dielectric guides as shown for two different $k_o a$ values in Fig. 1. One notes that as the separation distance is increased, the agree-

ment between the results based on coupled mode theories and our normal mode results becomes better, and that closer agreement is obtained for larger $k_o a$ values or when more power is confined within the core of the guide. This is because large $k_o a$ corresponds to more tightly-bounded field; hence, the coupling field is weaker and the coupled mode theory which is based on perturbation concept tends to be more accurate. It is worthwhile to point out that for certain combinations of $k_o a$ and $k_o d$ values such as for $k_o a = 1$ and $k_o d \leq 7.0$ only the dominant symmetric mode exists, so according to the exact normal mode theory, no back and forth exchange of propagating power takes place between guide A and guide B. On the other hand the approximate coupled-mode theory continues to predict the power exchange phenomenon. Another way of expressing the differences for the results based on different theories is shown in Fig. 9 where the percent differences between different coupled-mode theories and the normal mode theory are plotted against the normalized separation distances.

It can be seen that the coupled mode theory is surprisingly good (within 20%) in predicting the coupling length of two parallel dielectric slab guides even when the separation distance is relatively small and the confinement of guided power is relatively weak. Extrapolating our present results to other geometrics involving optical fibers or integrated optical guides, it is inferred that the coupling distances predicted according to the coupled mode theory are accurate to within 20% of the actual values if the symmetric and antisymmetric modes are both above cutoff. Finally, it should be noted that when the separation distance is small the transverse field configurations of the coupled guides (see Fig. 7) are significantly different than those assumed in the coupled mode theory.

REFERENCES

1. D. Marcuse, "Light Transmission Optics," pp. 417-421, Van Nostrand-Reinhold Co., New York (1972).
2. D. B. Hall, "Frequency Selective Coupling between Planar Waveguides," NELC Technical Note TN-2583, Naval Electronics Laboratory Center, San Diego, CA 92152 (1974).
3. S. E. Miller, Bell Sys. Tech. J. 33, 661 (1954).

FIGURE TITLES

Fig. 1. Geometry of the canonical problem.

Fig. 2. Normalized propagation constants as a function of normalized frequencies. The lowest order mode n = 1 has zero cutoff frequency.

Fig. 3. Normalized propagation constants as a function of normalized frequencies. All antisymmetric modes have cutoff frequencies.

Fig. 4. Normalized power in the core region of guides A and B as a function of the normalized longitudinal distance. The coupling length (defined as the length for which complete exchange of power in the cores of Guide A and Guide B occurs) is longer for less tightly bounded-fields.

Fig. 5. Normalized power in the core region of guides A and B as a function of the normalized longitudinal distance. P_C is the power in the core region of guide A or guide B as appropriate. P_T is the total guided power.

Fig. 6. Maximum normalized power in the core region of guide A as a function of separation distance of the two guides.

Fig. 7. Transverse electric field distribution across the two coupled guides.

Fig. 8. Normalized coupling length as a function of the normalized separation distance. Note that the coupling length ceases to exist for $k_o d < 7.0$ when $k_o a = 1.0$ according to the normal mode theory.

Fig. 9. Percent coupling length differences between normal mode theory and coupled mode theory as a function of normalized separation distance.

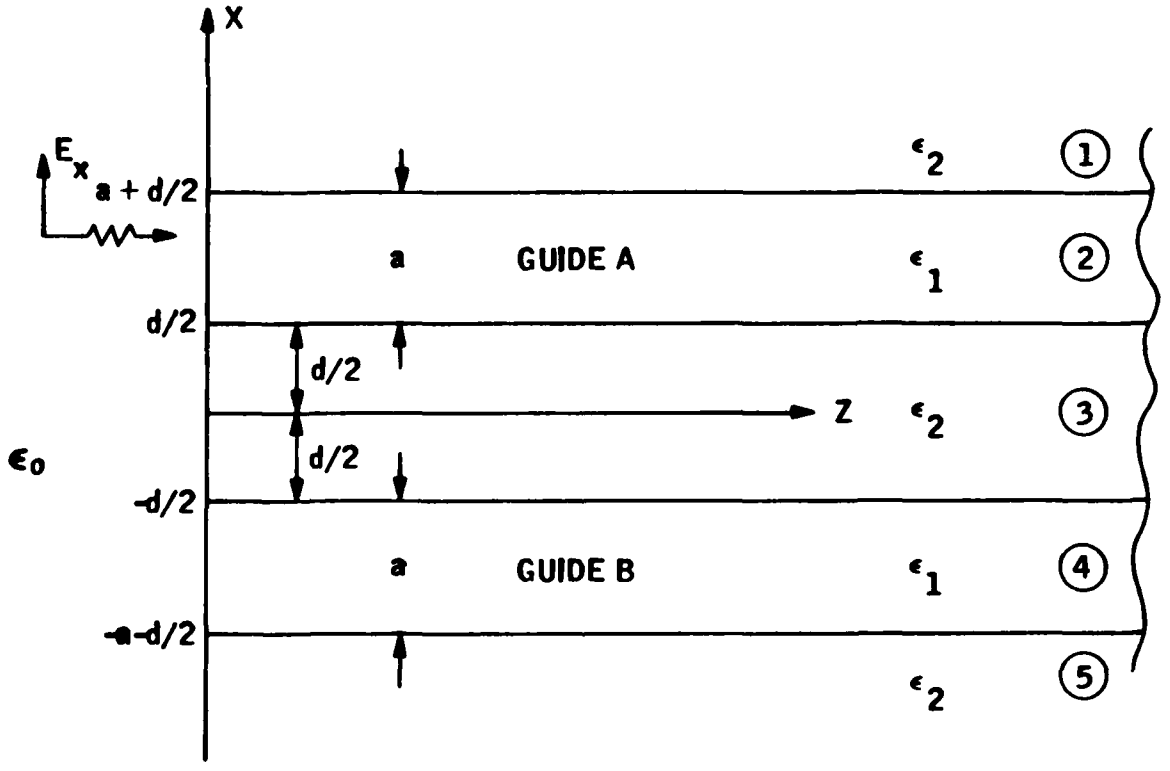
X
E_x
a + d/2
d/2
a
GUIDE A
d/2
Z
ϵ_0
d/2
-d/2
a
GUIDE B
-a-d/2
ϵ_2
ϵ_1
ϵ_2
ϵ_1
ϵ_2
1
2
3
4
5

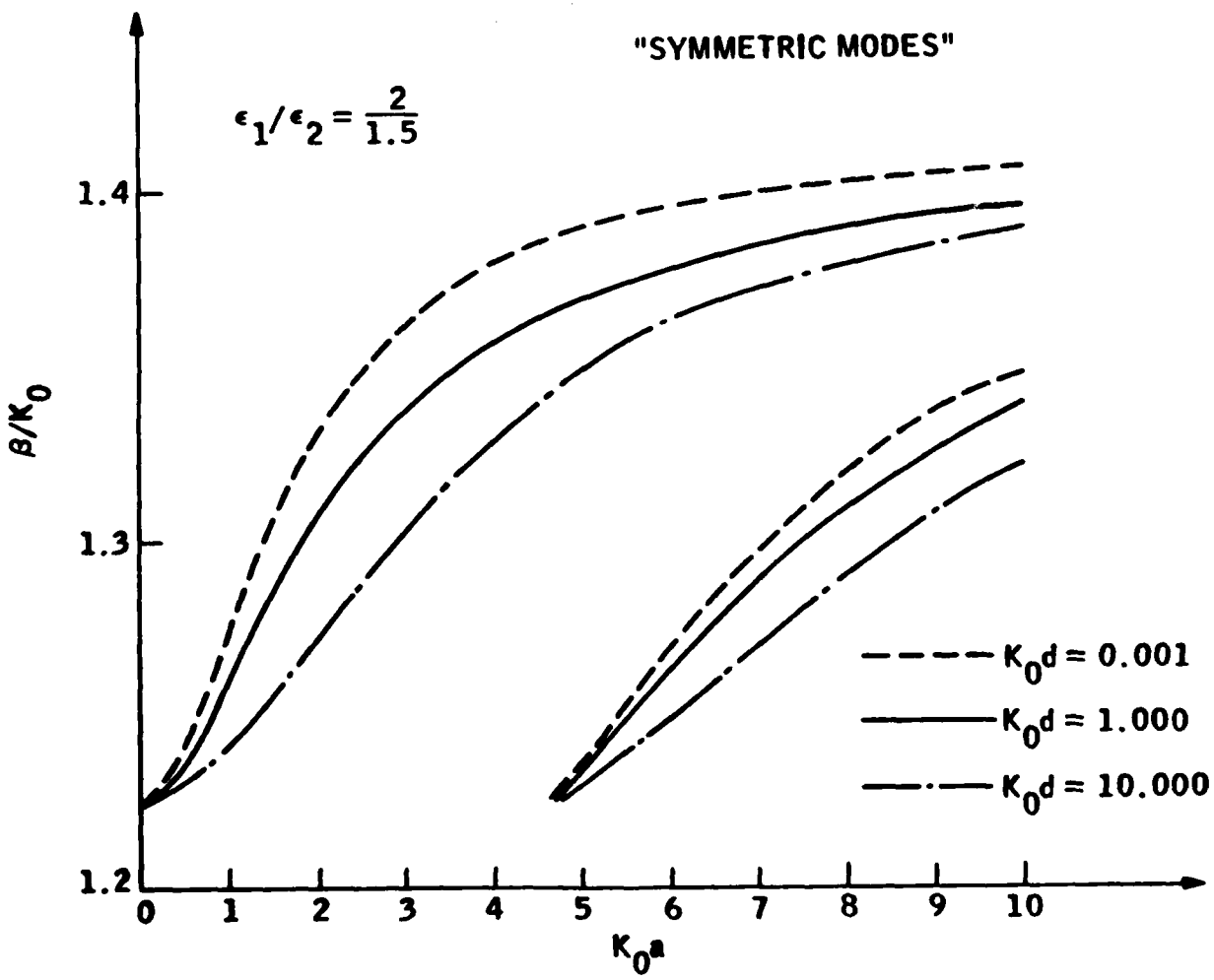
"SYMMETRIC MODES"
$\epsilon_1/\epsilon_2 = \frac{2}{1.5}$
1.4
1.3
1.2
β/K_0
0
1
2
3
4
5
6
7
8
9
10
K_0a
$K_0d = 0.001$
$K_0d = 1.000$
$K_0d = 10.000$

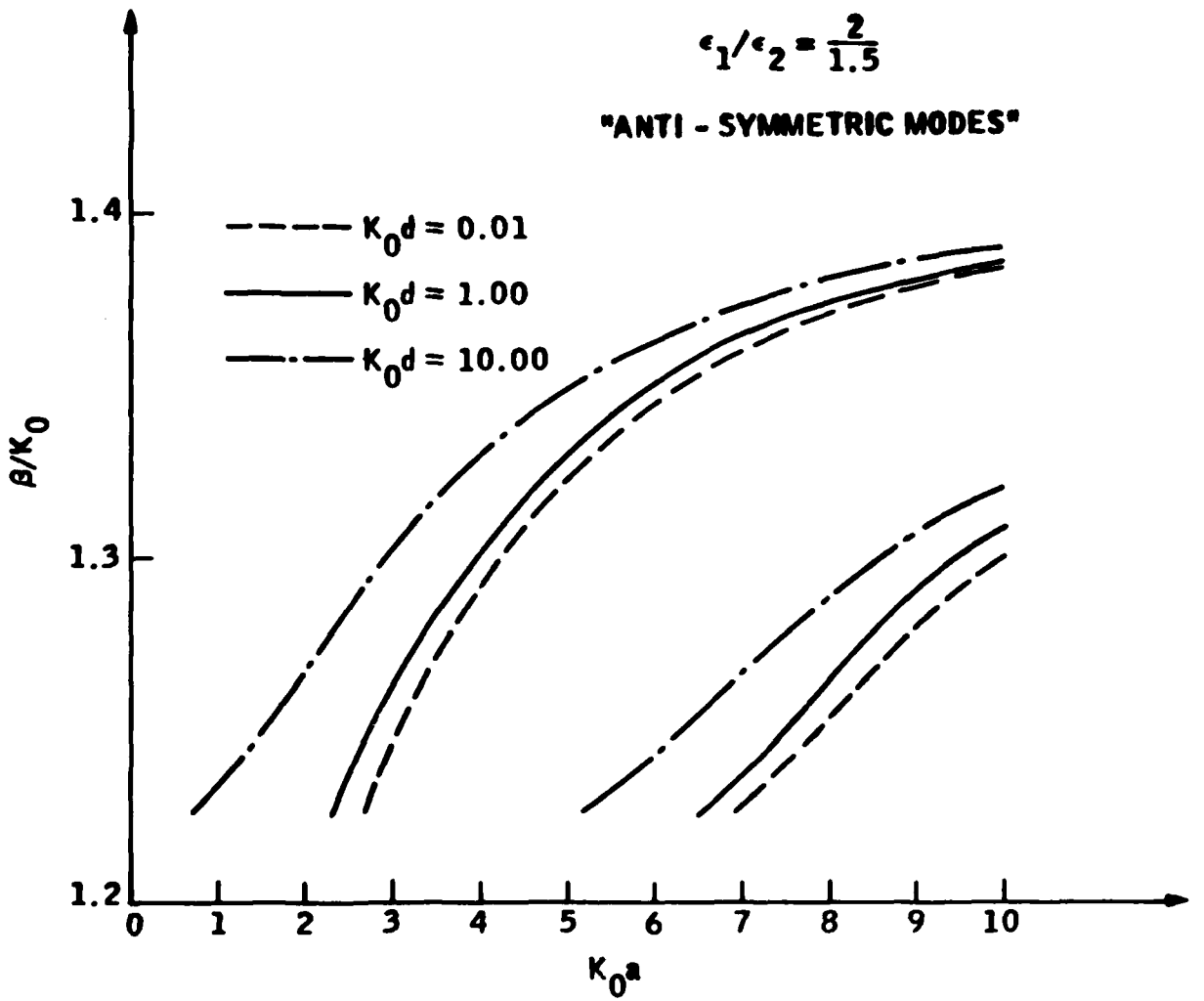
$\epsilon_1/\epsilon_2 = \frac{2}{1.5}$
"ANTI - SYMMETRIC MODES"
$K_0d = 0.01$
$K_0d = 1.00$
$K_0d = 10.00$
β/K_0
1.4
1.3
1.2
0
1
2
3
4
5
6
7
8
9
10
K_0a

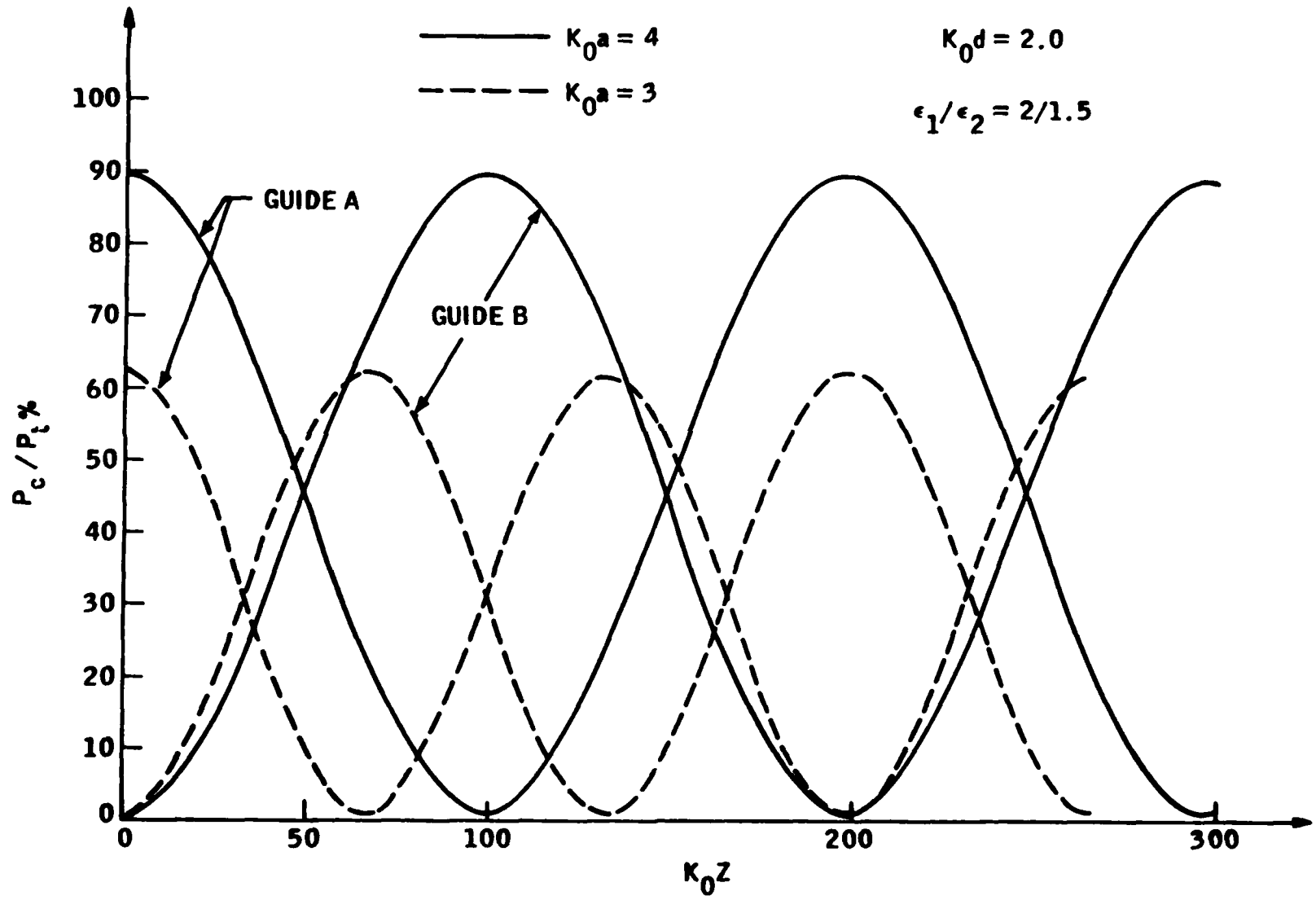
$K_0a = 4$
$K_0a = 3$
$K_0d = 2.0$
$\epsilon_1/\epsilon_2 = 2/1.5$
GUIDE A
GUIDE B
P_c/P_t %
100
90
80
70
60
50
40
30
20
10
0
0
50
100
200
300
K_0Z

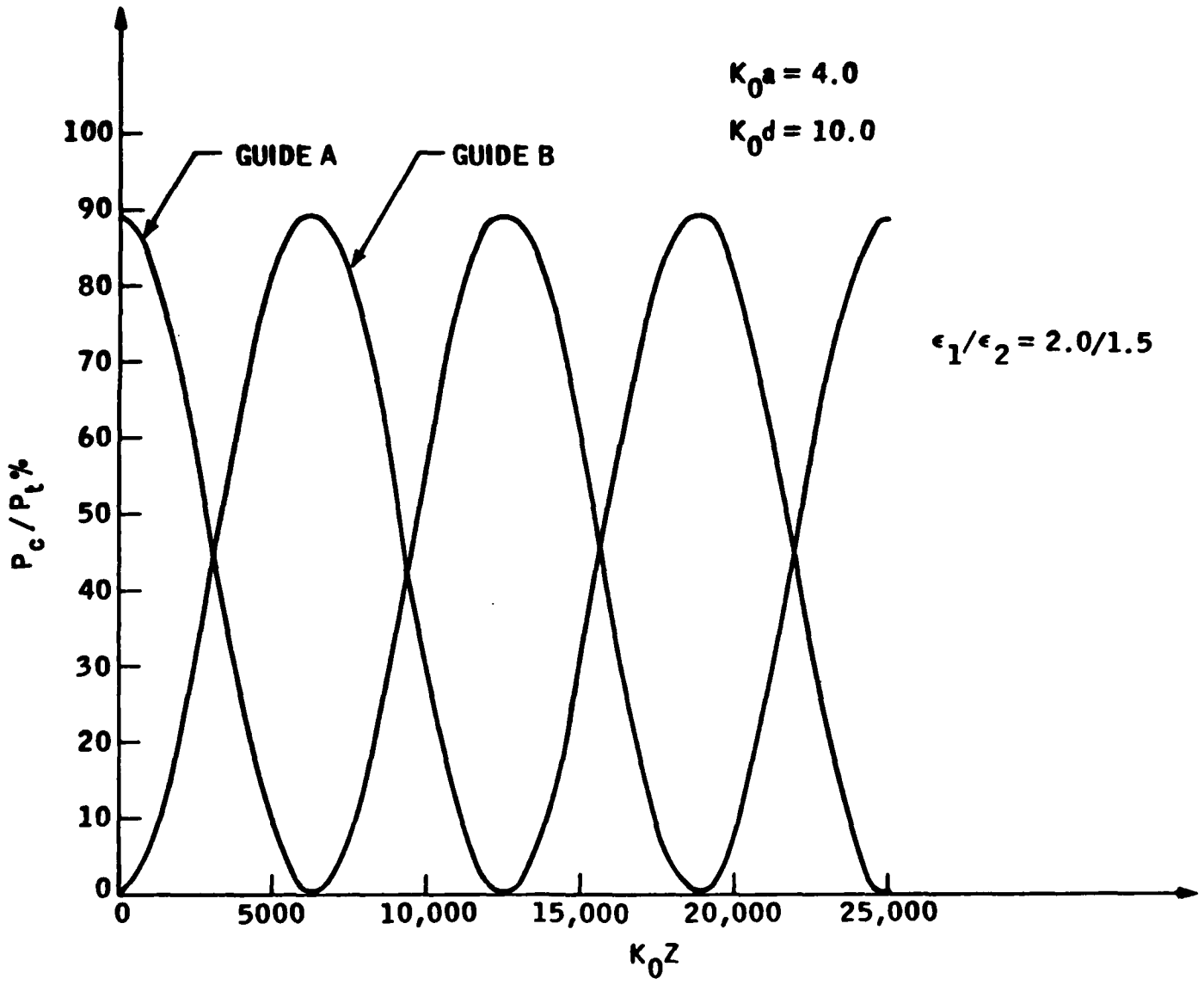
$K_0a = 4.0$
$K_0d = 10.0$
GUIDE A
GUIDE B
$\epsilon_1/\epsilon_2 = 2.0/1.5$
100
90
80
70
60
50
40
30
20
10
0
P_c/P_t%
0
5000
10,000
15,000
20,000
25,000
K_0Z

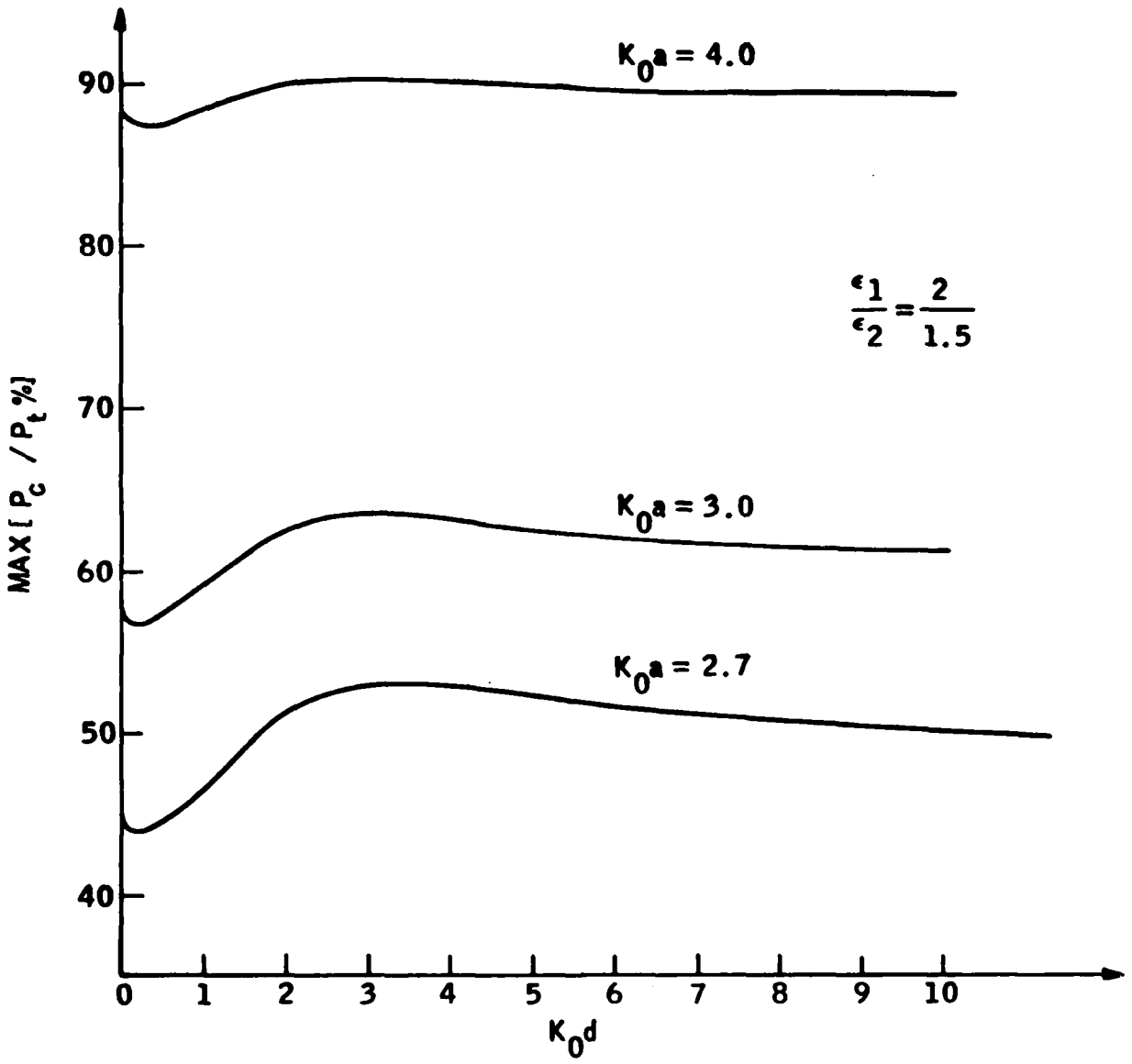
$K_0a = 4.0$
$K_0a = 3.0$
$K_0a = 2.7$
$\frac{\epsilon_1}{\epsilon_2} = \frac{2}{1.5}$
MAX [P_c / P_t %]
90
80
70
60
50
40
0
1
2
3
4
5
6
7
8
9
10
K_0d

Fig. 6

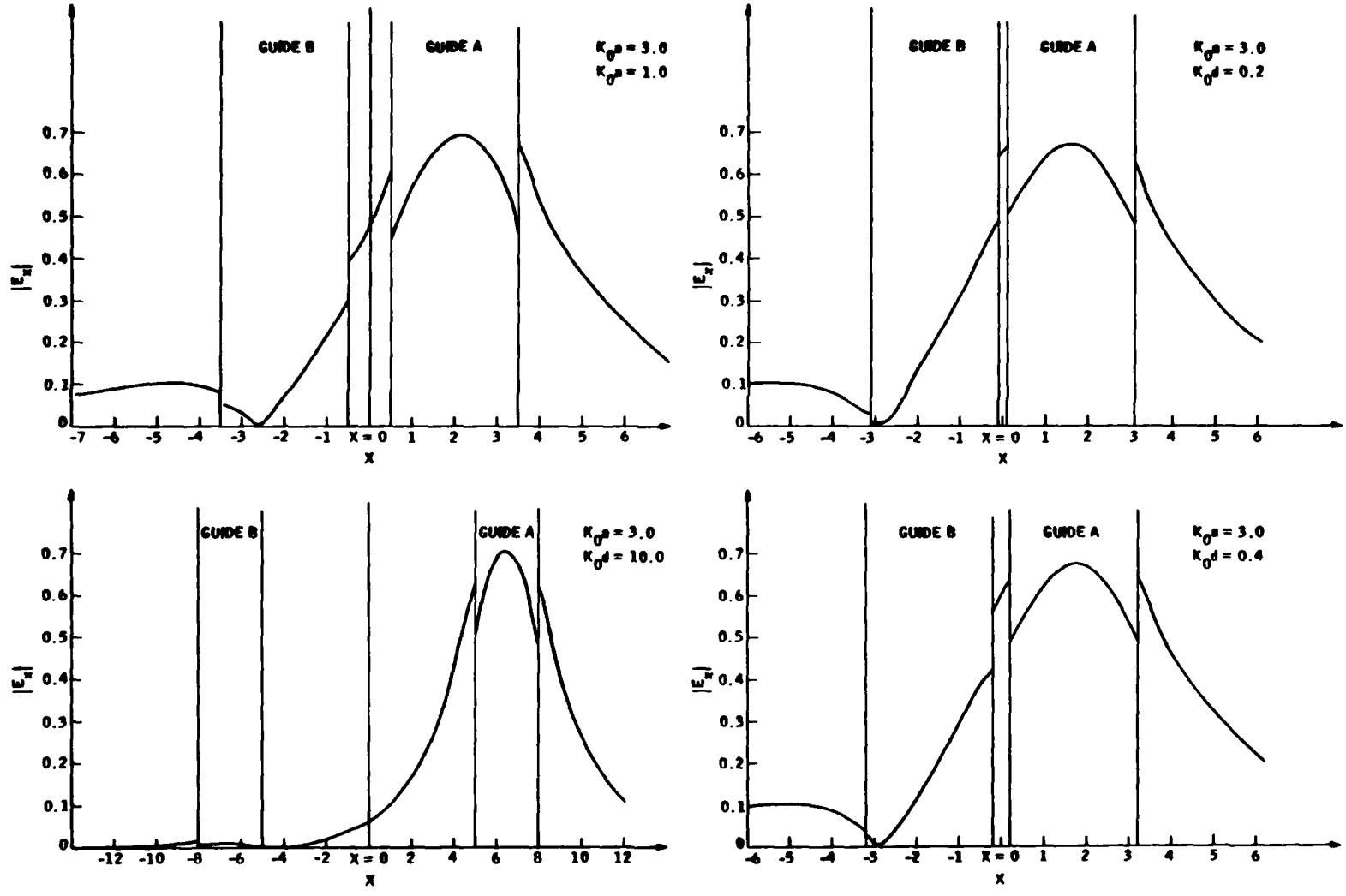
GUIDE B
GUIDE A
$K_0^a = 3.0$
$K_0^a = 1.0$
$|E_x|$
X
GUIDE B
GUIDE A
$K_0^a = 3.0$
$K_0^d = 0.2$
$|E_x|$
X
GUIDE B
GUIDE A
$K_0^a = 3.0$
$K_0^d = 10.0$
$|E_x|$
X
GUIDE B
GUIDE A
$K_0^a = 3.0$
$K_0^d = 0.4$
$|E_x|$
X

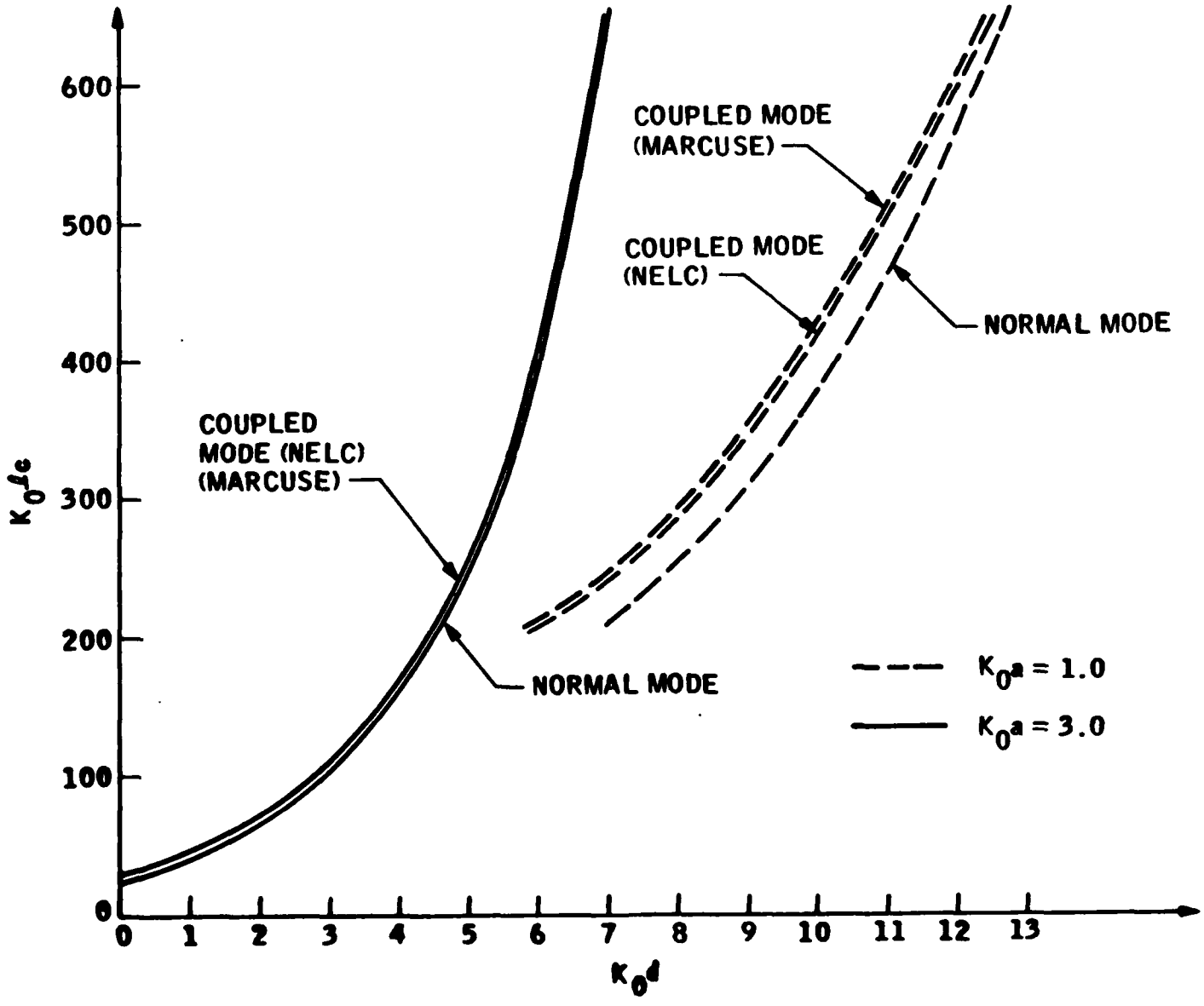
600
500
400
300
200
100
0
$K_0 d_e$
0 1 2 3 4 5 6 7 8 9 10 11 12 13
$K_0 d$
COUPLED MODE (MARCUSE)
COUPLED MODE (NELC)
NORMAL MODE
COUPLED MODE (NELC) (MARCUSE)
NORMAL MODE
$K_0 a = 1.0$
$K_0 a = 3.0$

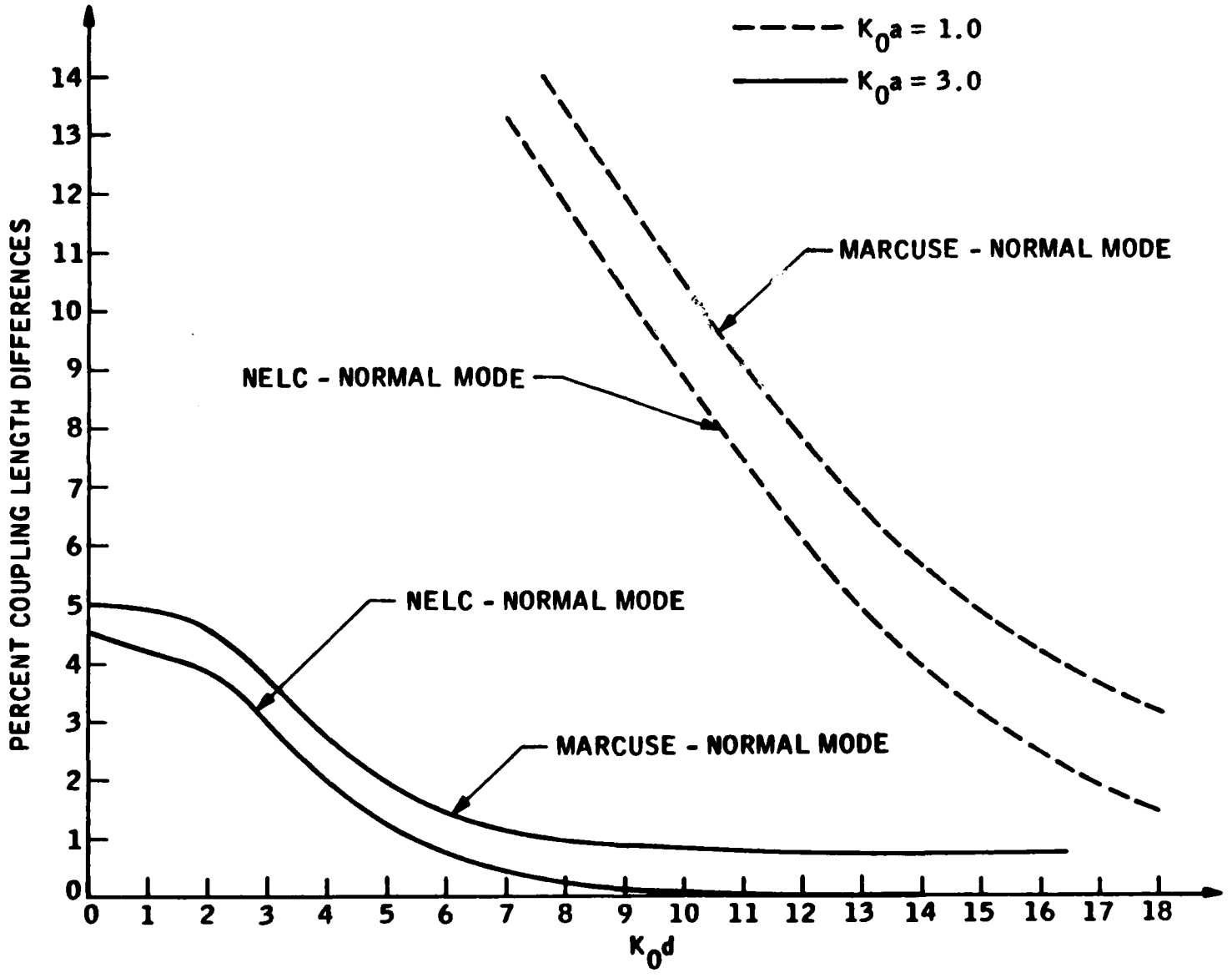
$K_0a = 1.0$
$K_0a = 3.0$
MARCUSE - NORMAL MODE
NELC - NORMAL MODE
NELC - NORMAL MODE
MARCUSE - NORMAL MODE
PERCENT COUPLING LENGTH DIFFERENCES
0 1 2 3 4 5 6 7 8 9 10 11 12 13 14
0 1 2 3 4 5 6 7 8 9 10 11 12 13 14 15 16 17 18
K_0d


DA
FIL
7